Computer & Robotics

Optimization of the DFIG Wind Turbine Controller Parameters by the Gray Wolf Algorithm

Mahyar Abbas Zadeh [a], Rezvan Abbasi [b,∗]

[a]Faculty of Electrical, Biomedical and Mechatronics Engineering, Qazvin Branch, Islamic Azad University, Qazvin, Iran

Abstract

The increase in the power generated by the wind has had effects on the performance of the power system in cases such as power quality, safety, stability, and voltage control. The wind turbines are used to generate electrical energy from wind. They can work in fixed or variable speeds. The asynchronous generator is directly connected to the grid for the fixed-speed wind turbines. In order to connect the DFIG (Doubly-Fed Induction Generator) to the grid, this machine must be able to integrate its generated power into the grid in a specific voltage (the grid voltage level). The main DFIG controlling method is the use of field-oriented vector control for regulating the rotor flux. The DFIG vector control consists of two main parts as grid side converter control and rotor side converter control. The rotor side converter is used to control the grid output power. This converter regulates the power factors in the terminals, and actually restores the generated power deviation from the reference power through the PID controllers, besides guaranteeing the stability of the induction generator. In the current study, the power was controlled through the determination of the PID optimal coefficient of the rotor and grid sides controllers and the gray wolf algorithm in the MATLAB software. In addition, the stability of the small signal of the grid equipped with the doubly-fed wind generator in the wind speed turbulence conditions was optimized to satisfy the required criteria in output active and reactive power of a DFIG. From the simulation results it is observed that the proposed controller yields better results when compared to other methods in literature in terms of performance index.

Keywords: Optimization, Doubly-Fed Induction, Generator, Wind Turbine, Gray Wolf Algorithm.

1.Introduction

From the initiation of the technology and invention of the windmill by the Iranians in 200 B.C, the first effort to use this energy was made that led to the next stage, which was the use of wind energy and wind machines only for the remote areas for which the fixed and trusted feeding was not important. The next phase was the development of the wind turbines through production and manufacturing the power generating wind turbines around the 1900s. The first wind power generator was made in Denmark in 1890. Then, a power generation system was installed in Russia in 1931. In those times, the number of wind turbines was gradually reduced since the diesel generators were developing, which were more economical and trustworthy. Regarding the limited sales of the oil during the WWI and WWII years, the wind turbines became the center of attention again, and it is estimated that until the next 20 years, the total installed capacity would increase up to 572733

megawatts. There are several reasons to use the DFIG wind turbines among which the increase in the turbine's energy absorption capacity, the decrease in mechanical structure tensions, the decrease in noise production, and controlling the active/reactive power can be named. However, absorption and conversion The classic method of doubly-fed induction generator active/reactive power control is the vector control method. For the implementation of the vector control method, the PI controller is used. The scalar control uses the equations in the stable conditions to calculate the domain and frequency (angular speed) of the voltage, current, and flux vector. But the vector control uses the dynamic equations for the calculation of the frequency, domain, voltage instantaneous position, current, and flux vector. The vector control can independently control the active/reactive power of the generator. This control method is based on the variables in the synchronous

∗ Corresponding Author Email: rezvanabbasi@yahoo.com

reference device. The d vector, if the synchronous reference is proportionate to the stator flux vector, lets the active/reactive powers be independent. During the last two decades, the power generation systems have been replaced by new energy resources such as wind in various European countries. The increase in wind energy usage, has had some effects on power system operation such as: quality of power, security, stability and voltage control (Pao et al., 2009). By connecting the wind turbine to the network, the load distribution model and dynamic properties of the network will change (Liu, 2017). For generation of electrical energy out of wind, the wind turbines can work at constant or variable speeds. In the case of constant speed turbines, the generator is directly connected to the network. The wind disturbance affects the power change and quality in such a system. Such turbines are designed so as to produce the maximum energy in just a synchronous speed. Any abrupt change in speed and power of wind causes the output power to oscillate. In variable speed turbines, the generator is controlled by power electronic devices. Utilization of power electronic devices in variable speed turbines, brings about the facility for the generator to have the ability of generating optimum power at any speed. The output power change of such turbines is controllable by electronic power devices. At the result, the problems of constant speed turbines are not experienced (Hau, 2007). There have been various control design efforts in the literature so far:

In a work done by (Zhao et al., 2007), a non-linear controller was used to limit the overcurrent in the rotor circuit. It has been shown in this study that due to the weakness on the exploitation point of the integral-proportional behavior, the current exceeds the allowable amount in the converters used in the wind turbines while an error occurs in the grid. Then a non-linear controller is designed, which shows that the converter currents remain in the allowable domain even in the low-voltage level.

(Nam et al., 2013) provides a continuous performance during the grid error for the wind turbine with a DFIG. In this method, the rotor side converter is blocked during the short circuit, and the rotor circuit is shorted out by CROWBAR circuit. In this state, the DFIG is transformed into an induction generator and starts to take the reactive power. The turbin continues to perform, and the grid side converter is controlled to generate reactive power. When the error is fixed, and the voltage and

frequency in the grid come to the normal state, the rotor side converter starts to operate and performs normally.

In this method, if the power grid to which the wind turbine is connected, is weak, the GSC cannot generate enough reactive power required for both the grid and generator, since its power capacity becomes 25 to 30% of the generator's nominal power. It can lead to voltage instability and consequently, the RSC cannot be started, and the wind turbine would remain disconnected from the grid.

(Kristalny et al., 2006), solves this problem by the use of a reactive power compensator. The authors of this study have investigated the use of a STATCOM to help with the continuous performance of a wind farm with DFIG during the grid error. The grid used in this study was a single machine connected to an infinite bus so that there was no consistency between the STATCOM and the wind farm for controlling the reactive power. (He et al., 2015) has provided a method for continuous operation of DFIG during a short-circuit in the grid. In this method, through the creation of a bypass in the rotor by a resistance which is connected to the rotor's winding, the current in the rotor has been limited. Since the generator and the converter remained connected to the grid, the synchronism performance was maintained during the error and after it, and the normal performance was continued right after fixing the error. (Battista et al., 2000), reduced the overcurrent in the circuit through the use of Fuzzy controller in the RSC. In fact, this study has used RSC controlling model instead of the integral-proportional controller. Then, the results of the simulation using this model have been compared with those obtained from the integral-proportional controller.

In research done by (Pradhan et al, 2018) the work performed by (Kristalny et al., 2006), has been improved. A consistent reactive power control model between the STATCOM and the wind turbine has been created by the use of the neural network. (Johnson et al., 2005), implements a DFIG-consistent voltage control for continuous operation in the grid. This method is based on the fact that both GSC and RSC of the DFIG are used in a consistent manner. The idea is like that the RSC is considered as the reactive power source, while the

GSC is considered as a reactive power supply when the protective system is activated. As a result, the RSC is locked. (Hwas et al., 2012) instead of using a 3-phase FSC, has used 3 single-phase converters which are serially connected to the grid. When an error occurs in the system, the converter located in the phase with error, injects a little voltage to that phase, so that the voltage seen by the generator becomes higher than the error voltage and the error current becomes limited. (Kahla et al., 2017) presents a multi objective grey wolf optimization (MOGWO) of fuzzy sliding mode controller in order to maximize the power captured by wind turbine. The proposed strategy of (Alhato et al., 2020) is a combination of the Lyapunov theory and metaheuristics algorithms, which has been considered to identify the optimal gains of the STA-SOSM (Super Twisting Algorithm-second-order sliding mode) controllers. Practical application in a Distributed Power Generation System (DPGS) with energy storage is considered by designing an Adaptive Fuzzy PID (AFPID) controller using the suggested SGWO(Simplified Grey Wolf Optimizer) method for frequency control by (Padhy et al., 2021). An enhanced control strategy for both rotor side and grid side converters is also presented using the ABC and GWO (Soued et al., 2019).

One of the most important parameters of power quality in the wind turbines is the voltage regulation. The main method of DFIG control is the use of vector control for regulating the rotor flux. The DFIG vector control consists of two main parts as Grid Side Converter (GSC) and Rotor Side Converter (RSC). The rotor side converter is used to control the network's output power. This converter regulates the power factor in the terminals and actually, restores the required power through the ratio of generated power deviation from the reference power by the PID controller, as well as ensuring the stability of the induction generator. In the current study, it was sought to perform the voltage and power control through the determination of optimum PID coefficients of rotor and grid side controllers by the use of gray wolf algorithm in the MATLAB Software, and optimize the small signal stability grid with doubly-fed wind generators in the turbulent conditions.

2. Statement of the Problem

Based on the IEC 61400-22, in case multiple dispersed generation sources are used in the grid and they are connected to a feeder, the voltage size change resulting from all the sources must be considered. Therefore, the precise loading distribution of the system is vital. Investigation of the stable state of the voltage on the binding point of the dispersed generation sources to the distribution grid feeders is one of the fundamental parameters of such grids. According to the standard, this amount should not exceed 2% in the medium voltage networks, so that the changes in the low-voltage network would not be more than 10%. For the modes in which the power generation of the dispersed generation sources is maximum and the power consumption of the network loads is minimum, the voltage size change on the binding point would be minimum. The average voltage size of each binding point should not exceed 5% of the nominal voltage so that by the use of medium-voltage, tap changer`s transformation to the low-voltage can be compensated. The binding point voltage size around the medium voltage should not exceed 3% of the nominal voltage in order for the low-network voltage to remain lower than 10%.

Regarding the increasing trend of the use of new energies, especially that of wind, in the generation of electricity, improving the quality of the generated power by the wind turbines is necessary. The wind turbines must be able to generate the required power in any environmental conditions or any other given conditions. In this regard, the power quality phenomena are among the important issues in wind turbines` performance.

One of the most used generators in the wind turbines are the doubly-fed induction generators. These generators have been more focused in recent decades due to their advantages over other generators. Among the main advantages of these generators, the independent controlling of the active/reactive powers, speed control ability, and lower costs of the electronic equipment can be noted. The DFIG

equipped with the controller provides the possibility of independent controlling of the active-reactive power, and its main advantage is that one-third of the generator specific power flows through the inverters, which makes the converter smaller and more economical, and simultaneously increases the efficiency. In the current study, we have dealt with the optimization of the small signal stability and the signal in the connection point of the wind farm to the power grid through the use of gray wolf algorithm for determination of PID controllers` coefficients of the large converters in doubly-fed induction generators, as well as the investigation of this algorithm's efficiency, compared to other algorithms.

3. Induction generator modeling

The induction generators are divided into two categories of variable speed two stimulation and constant speed squirrel cage induction generators. For modeling the induction generators, two dynamic models are used, in which the first one is based on space vector model and the second one is based on d-q axis inferred from space vector. The mentioned models are close to each other and in the sequel, the induction generator is synthesized using these routes:

$$V_{abcs} = r_s i_{abcs} + \rho \lambda_{abcs} \tag{1}$$

$$V_{abcr} = r_r i_{abcr} + \rho \lambda_{abcr} \tag{2}$$

3.1. Space Vector Model of Two Excitation Induction Generators

In space vector model of induction generators, it is assumed that the induction generator is Symmetrical and has three Balanced Phases and the magnetic core is linear and the loss is minor. As a whole space vector model is composed of three sets of voltage, linkage flux and motion equations. Stator and rotor generator voltage equations in optional reference frame are as follows:

$$\begin{cases} \vec{v}_s = R_s \vec{i}_s + p\vec{\lambda}_s + j\omega\vec{\lambda}_s \\ \vec{v}_r = R_r \vec{i}_r + p\vec{\lambda}_r + j(\omega - \omega_r)\vec{\lambda}_{rs} \end{cases} \tag{3}$$

The terms $\omega\vec{\lambda}_x$ and $j(\omega - \omega_r)\vec{\lambda}_r$ in the right side of the equation (3) indicate the Induced voltage speeds in arbitrary speed reference frame ω. The second terms indicate the Stator and rotor linkage flux $\vec{\lambda}_x$ and $\vec{\lambda}_r$.

The third equation is the machine motion equation which describes the dynamic behavior in mechanical speed of the rotor by two terms of mechanical and electromagnetic torque.

$$J\frac{d\omega_m}{dt} = T_c - T_m \tag{4}$$

$$T_e = \frac{3p}{2} Re(j\vec{\lambda}_s \vec{i}_s) = -\frac{3p}{2} Re(j\vec{\lambda}_r \vec{i}_r) \tag{5}$$

The above equations form the space vector model of the induction generator. Generator model in optional reference frame and rotation in space with optional speed is illustrated in figure (1).
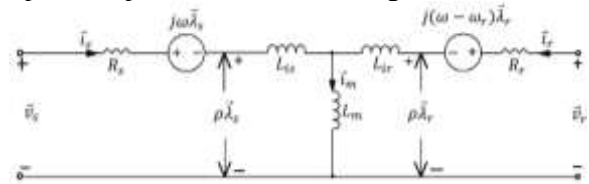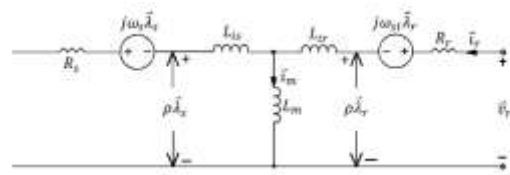

Fig 1: equivalent Circuit of the space vector of an induction generator in optional reference frame (Rajesh et al., 2017)

Considering the model inferred in synchronous frame of figure (2) in which ω_s is the synch speed and ω_{sl} is the generator Angular slip frequency, we have:

$$\begin{cases} \omega_s = 2\pi f_s \tag{6} \\ \omega_{sl} = \omega_s - \omega_r \tag{7} \end{cases}$$
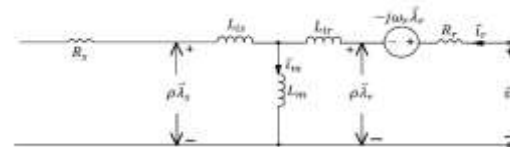

(a) IG model in the synchronous frame

(b) IG model in the stationary frame

Fig 2: Space vector model of induction generator in synchronous and constant reference frame (Yang et al. 2017)

3.2. d-q Reference Frame Model

The d-q model in induction generator can be inferred by decoupling the space vectors of d and q axis.

$$\vec{v}_s = v_{ds} + jv_{qs}; \vec{i}_s = i_{ds} + ji_{qs}; \vec{\lambda}_s = \lambda_{ds} + j\lambda_{qs} \quad (8)$$

$$\vec{v}_r = v_{dr} + jv_{qr}; \vec{i}_r = i_{dr} + ji_{qr}; \vec{\lambda}_r = \lambda_{dr} + j\lambda_{qr} \quad (9)$$

By inserting (9) in (6) and separating real and imaginary parts in two sides of equation, the d-q voltage equations in induction generator is inferred as follows:

$$v_{ds} = R_s i_{ds} + p\lambda_{ds} - \omega\lambda_{qs} \quad (10)$$

$$v_{qs} = R_s i_{qs} + p\lambda_{qs} + \omega\lambda_{ds} \quad (11)$$

$$v_{dr} = R_r i_{dr} + p\lambda_{dr} - (\omega - \omega_r)\lambda_{qr} \quad (12)$$

$$v_{qr} = R_r i_{qr} + p\lambda_{qr} + (\omega - \omega_r)\lambda_{dr} \quad (13)$$

And similarly the d-q Linked Flux Equations Will be achieved:

$$\lambda_{ds} = (L_{ls} + L_m)i_{ds} + L_m i_{dr} = L_s i_{ds} + L_m i_{dr} \quad (14)$$

$$\lambda_{qs} = (L_{ls} + L_m)i_{qs} + L_m i_{qr} = L_s i_{qs} + L_m i_{qr} \quad (15)$$

$$\lambda_{dr} = (L_{lr} + L_m)i_{dr} + L_m i_{ds} = L_r i_{dr} + L_m i_{ds} \quad (16)$$

$$\lambda_{qr} = (L_{lr} + L_m)i_{qr} + L_m i_{qs} = L_r i_{qr} + L_m i_{qs} \quad (17)$$

And electromagnetic torque T_e in equation (5) is inferable by the Linked flux and d-q currents.

The equations (11) to (13) and motion equation of (8) illustrate the d-q induction generator model equivalent to the circuit of figure (3) in optional reference frame. For inferring the d-q model in constant and synch reference frame, the optional frame speed ω in generator can be chosen to be the stator synch frequency ω_s and zero respectively.

(a) d-axis circuit
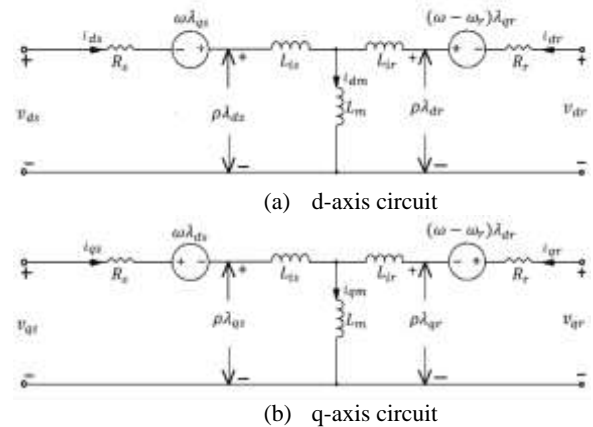

(b) q-axis circuit

Fig 3: d-q axis model of induction generator in optional reference frame
(Yang et al. 2017)

4. Gray Wolf Algorithm

In gray wolf groups, the leaders are a male and a female called alpha. In this section, the mathematical model of social hierarchy, tracking, siege and attack on the prey is presented. Then the GWO (Gray Wolf Optimizer) algorithm is detailed. During design, in order to model the social hierarchy of wolfs, the most suitable solution is regarded as alpha and the second and third one as beta and gamma respectively. The rest of candidate solutions are called omega. In the algorithm, the hunting process (optimization) is guided by alpha (α), beta (β) and gamma (δ). The omega (ω) wolfs obey these three groups.

4.1. Bait Siege

As mentioned above, the gray wolfs siege the bait along the hunt. In order to model this behavior mathematically, the following equations are presented:

$$\vec{D} = \left| \vec{C}.\overrightarrow{X_p}(t) - \vec{X}(t) \right| \quad (18)$$

$$\vec{X}(t+1) = \overrightarrow{X_p}(t) - \vec{A}.\vec{D}$$

In which t represents the current repetition. *A, C, X_p* and *X* represent the coefficient vectors, the prey position vector and the position of a gray wolf respectively. The vectors *A* and *C* are computed as follows:

$$\vec{A} = 2.\vec{a}.\overrightarrow{r_1}(t) - \vec{a} \quad (19)$$

$$\vec{C} = 2\overrightarrow{r_2}$$

In the above equations, *a* is linearly decreased from 2 to zero during epochs. The variables r_1 and r_2 indicate the random vectors in a limited period. As an example two and three dimensional location vectors and some probable neighborhood is illustrated in figure (4).
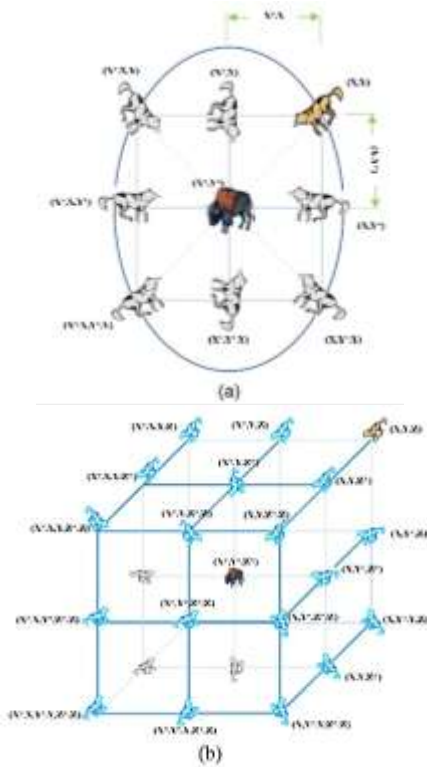

Fig 4: Two and three dimensional location vectors and the next probable position of them (Osman et al. 2015)

As seen in the figure, a gray wolf located in coordinates (X,Y), can change his position considering the position of the bait or (X^*, Y^*). The different locations around the best operator can be computed regarding its current position and changing and tuning the vectors *A* and *C*. It should be noted that the random vectors r_1 and r_2 let the wolfs access any position between the illustrated points in the figure; so, a gray wolf can change his location inside the space around the bait randomly and using the following equations:

$$\overrightarrow{D_\alpha} = |\overrightarrow{C_1}.\overrightarrow{X_\alpha} - \vec{X}|$$
$$\overrightarrow{D_\beta} = |\overrightarrow{C_2}.\overrightarrow{X_\beta} - \vec{X}|$$
$$\overrightarrow{D_\delta} = |\overrightarrow{C_3}.\overrightarrow{X_\delta} - \vec{X}| \qquad (20)$$
$$\overrightarrow{X_1} = \overrightarrow{X_\alpha} - \overrightarrow{A_1}.(\overrightarrow{D_\alpha})$$
$$\overrightarrow{X_2} = \overrightarrow{X_\beta} - \overrightarrow{A_2}.(\overrightarrow{D_\beta})$$
$$\overrightarrow{X_3} = \overrightarrow{X_\delta} - \overrightarrow{A_3}.(\overrightarrow{D_\delta})$$

$$\vec{X}(t+1) = \frac{\vec{X}_1 + \vec{X}_2 + \vec{X}_3}{3}$$

Such a concept is generalizable in an *n* dimensional search space. In this case, the gray wolfs move about the best solution in dimensions more than a cube.

4.2. Hunting

The hunting process is usually guided by alpha. The beta and delta wolfs might also sometimes take part in hunting. Unfortunately, in an abstract search space there is no idea about the optimal location (bait). For the purpose of mathematical modeling of the prey of wolves, it is assumed that alpha is the best solution and beta and delta have better knowledge about the potential location of the prey; so, three of the best solutions are saved and the other search elements such as omega wolves are obliged to update their location regarding the best search locations. Figure (5) shows the procedure of updating a search element in a two dimensional space regarding the location of alpha, beta and delta.
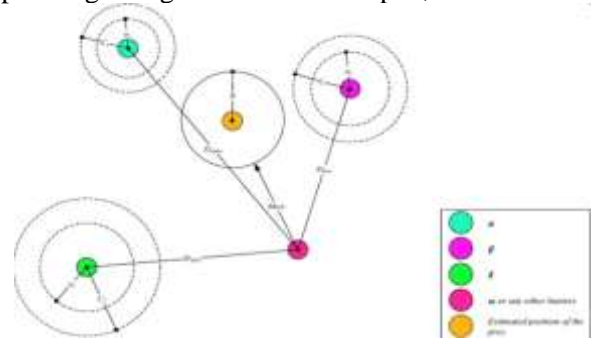

Fig 5: location update in GWO algorithm (Rajesh et al., 2017)

4.2.1. Prey Attack

For modeling the approaching to the prey, A is reduced. It should be noted that the oscillation range of A is reduced by a; In other words, A is a random quantity in the range of [0,2a]; while a is reduced from 2 to zero during epochs. As long as the random quantity of A is in the range, the next location of the operator can be at any location between its current and the prey locations. The above figure shows that the absolute value of A less than one, obliges the wolves to attack the prey.

4.2.2. Searching the Prey (Identification)

Gray wolfs usually start the search regarding the location of alpha, beta and gamma. The get distant from each other for seeking the prey and get close and cooperate for attacking it. for modeling such a divergence mathematically, the vector A is used with random quantities between 1 and -1 in order to cause the search operator to diverge and get distant from the prey. This procedure, shows the identification process and lets the GWO algorithm to perform the search globally. Figure (6) shows that A makes the wolves to diverge from the prey and find a more suitable one.

(b)   (a)
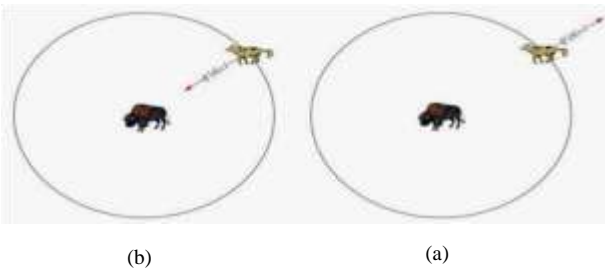
Fig 6: attacking the prey versus bait search (Osman et al. 2015)

- Initialize the grey wolf population X_i (i= 1,2, ..., n)
- Initialize a, A, and C
- Calculate the fitness of each search agent
- X_a = the best search agent
- X_β = the second best search agent
- X_δ = the third best search agent
    * While (t < Max number of iterations)
        * For each search agent
            * Update the position of the current search agent by above equations
        * end for
        * Update a, A, and C C
        * Calculate the fitness of all search agent
        * Update X_a, X_β and X_δ
        * t = t+1
    * end while
- return X_a

Fig 7: The pseudo code for the GWO algorithm
(Osman et al. 2015)

5. Wind Turbine Modeling

In order to investigate the efficiency of the proposed method for voltage control, a power distribution system including a 9-megawatt wind farm which consisted of 6 1.5-megawatt turbines, was designed in the MATLAB Software. These turbines were connected to a 120-kilowatt power grid through a transmission line with a 30-kilometer length. A load of 2300 V, and 2 MV including a load of a motor consisted of an induction motor of 1.68mW, and power coefficient of 0.93. The wind

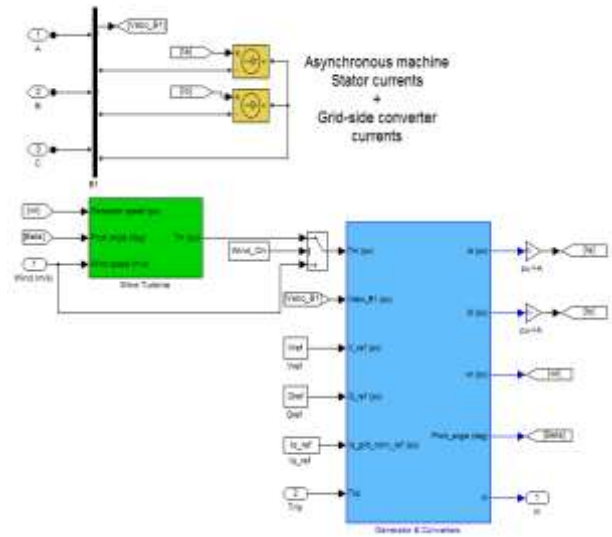turbine model designed in MATLAB Software has been shown in Figure (8).

Fig 8: Wind turbine model in MATLAB

6. Statement of Problem Regarding Optimization

The vector control in the vector field orientation was based on a procedure that enabled independent control of active/reactive powers, modeling the analyses done for optimization of the transient performance with regards to the stator flow orientation with the PI controller. The RSC was used to control the actual power of DFIG for extracting the wind power and maintenance of the terminal voltage based on the reference value. The active power was controlled by the v_{qr} and v_{dr} components which were the rectangular and vertical components of rotor voltage, respectively, which controlled the active power and voltage by application of the RSC. The simplified form of RSC has been depicted in figure (9):
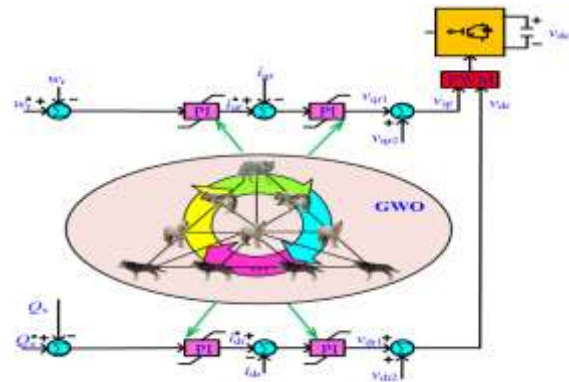

Fig 9: Flowchart of power control in DFIG (Osman et al. 2015)

In order to optimize the dynamic response and reduce the overshoot and setting time of controller response to the wind speed changes and reference active/reactive power generated by the generator, it was required to select optimal coefficients for the PI controller, and the gray wolf algorithm was suggested due to the supervised and targeted search. In order to do so, it was required to minimize the PID setting time and control error rate based on the design problem conditions. The inequalities were the physical limitations of the coefficients in designing and building the PI controllers, and the F(x) function was the optimization objective function and based on the importance of the three variables of the control in RSC including the machine speed, active reference power, and reactive reference power, it was necessary to consider the control variables` deviation from the reference value as the optimization objective function, and define it as the control error absolute value integral. In this regard, three types of objective function of optimization have been defined.

Therefore, the proposed search algorithm flowchart has been as follows:

- Setting the initial parameters of the search algorithm
- Random construction of the initial population (PI control coefficients) of the wolves for the evaluation of the position of each wolf and computation of its competency (F objective function)
- Identification of the best wolf as the alpha wolf, and the second and third wolves as the beta and delta wolves
- Iteration of the 6th to 12th phases as long as the stop condition is not met
- Iteration of phases 7 to 11 for each wolf
- Determination of three new positions for the wolves based on the position of the alpha, beta, and delta wolves
- Updating the wolf's position based on the three obtained positions
- Computation of the competence of the new wolf
- If the new wolf be more competent than the alpha wolf, and if it not be more competent than beta and delta wolves, choose the alpha wolf
- If the stop condition is not met, go to stage 5, otherwise, go to the finish

Now, in the next chapter, the optimal coefficients of PI controller for each F mode has been obtained with the gray wolf algorithm, and the results have been compared with those of other famous search algorithms such as the Genetic Algorithm(GA) (Vieira et al. 2010) and the particle swarm optimization (PSO) Algorithm (Bekakra et al.2013) to evaluate the importance of determination of the optimization objective function in controlling the DFIG generator power, voltage, and speed.

7. Simulation and Analysis of the Results

In this section, the results of the simulation of PI coefficients optimization for each of the three objectives have been evaluated.

7.1. Evaluation of the Simulation Results for Mode 1

In this section, the absolute error integral of the generator speed to the reference speed has been evaluated in a wind speed of 10 m/s and the nominal power has been considered as the PI controller optimization function. The convergence chart of the gray wolf, PSO, and genetic algorithms with similar settings and maximum iteration of 30 and 100, respectively, were as below. In this regard, the speed error was a minimum value of 0.55 in the 36th iteration for the gray wolf algorithm, 0.55 in the 53rd iteration for PSO algorithm, and 0.58 in the genetic algorithm. In fact, the genetic algorithm was stuck at the local minimum.
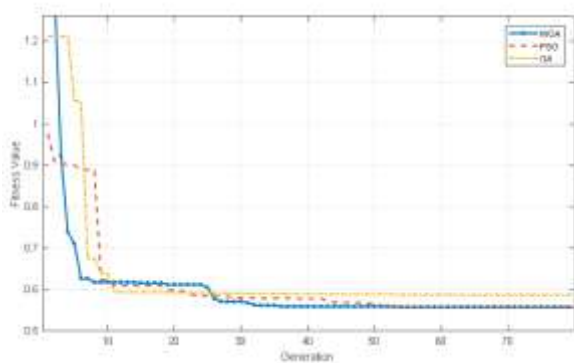
Fig 10: The three algorithms` convergence in mode 1

Also, the chart of the response to the generator speed with optimum coefficients for all three methods and the default coefficients of the algorithm was as below. In this regard, the gray wolf algorithm had a shorter setting time, and after 9 seconds, the speed tended to the nominal value, while the genetic algorithm had a relatively slow setting time, which was 18 seconds.
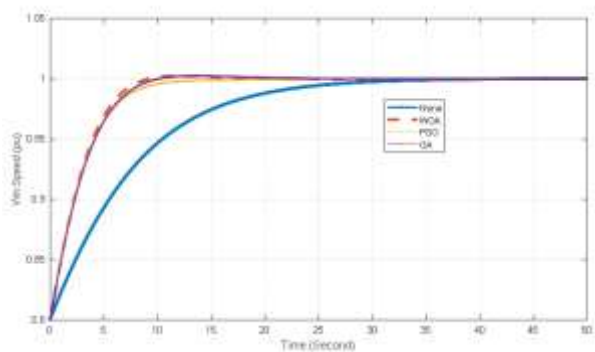

Fig

Fig 11: Generator`s speed chart in mode 1

The chart of the step response of the power generated by RSC was as below. Similar to the previous section, the gray wolf algorithm had a shorter setting time and had tended to nominal per unit in the fixed speed of wind in 16 seconds. The genetic algorithm setting time has been longer than that of PSO algorithm.
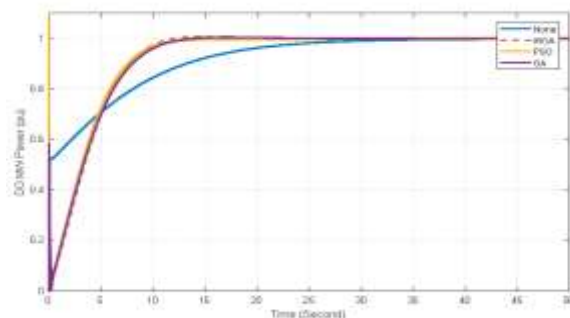

Fig 12: Generator reactive power chart in mode 1

The step response of the reactive power generated with optimum coefficients was as below. In this regard, the gray wolf algorithm had slower damping compared to the other algorithms, and the default coefficients of PID controllers have had the minimum setting time in this algorithm. In order to improve the controllers` setting time by the intelligent search algorithm, it was necessary to apply the reactive power control error in the objective function of optimization.
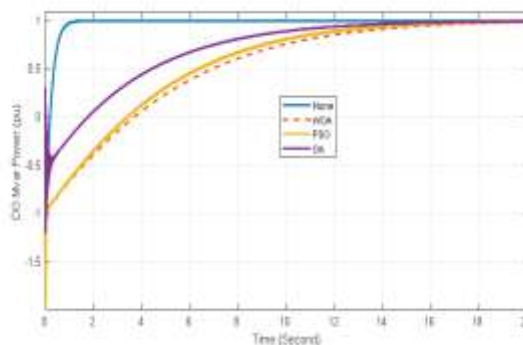

Fig 13: Generator`s reactive power in mode 1

7.2. The Results of Simulation for Mode 2

In this section, the sum of generator`s speed`s absolute error integral to the reference speed and the reactive power`s control error has been chosen as the PI control optimization objective function. The convergence chart of the gray wolf, PSO, and genetic algorithms with similar settings and maximum iteration of 30 and 100, respectively, were as below. In this regard, the speed error was a minimum value of 0.69 in the 18th iteration for the gray wolf algorithm, 0.71 in the 23rd iteration for PSO algorithm, and 0.76 in the genetic algorithm. In fact, the genetic algorithm was stuck at the local

minimum. Moreover, the genetic algorithm, due to the untargeted random search and broader search space, has demanded a larger number of iterations, and finally, in the 60th iteration, it has been stopped in the local minimum. However, the proposed algorithm has gotten out of the local optima trap in the 13th iteration, and according to the figure (14), it has tended towards the global optimum of the sum of error integral.
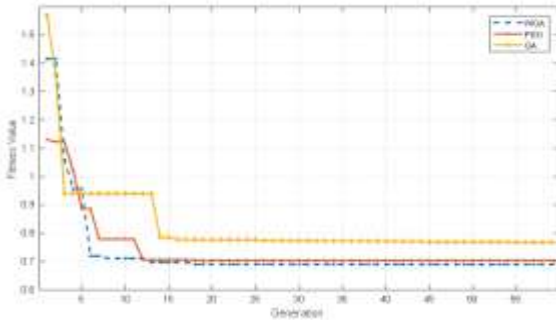

Fig 14: Three algorithms` convergence in mode 2

Also, the chart of the response to the generator speed with optimum coefficients for all three methods and the default coefficients of the algorithm was as below. In this regard, the gray wolf algorithm had a shorter setting time, and after 18 seconds, the speed tended to the nominal value, while the genetic algorithm had a relatively slow setting time which was 24 seconds.
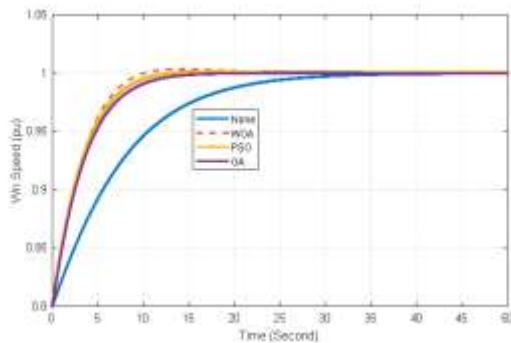

Fig 15: Generator`s speed chart with fixed wind speed in mode 2

The chart of the step response of the generated power was as below. Similar to the previous section, the gray wolf algorithm had a shorter setting time and had tended to nominal per unit in the fixed speed of wind in 22 seconds. The genetic algorithm setting time has been longer than that of PSO algorithm.
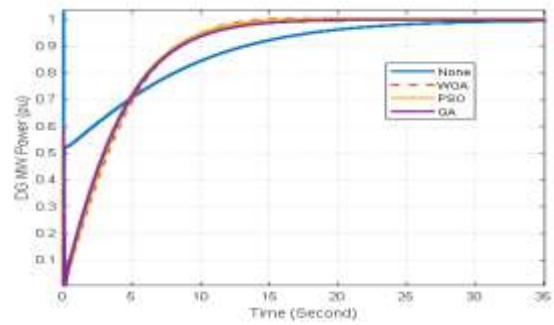

Fig 16: Generator`s reactive power with fixed wind speed in mode 2

The chart of the step response to the reactive power generated with the optimum coefficients was as below. In this regard, the gray algorithm had a lower initial fluctuation compared to the other two search algorithms, and the damping of the gray and PSO algorithms was almost the same. It should be noted that due to the application of the reactive power control error in the optimization, the reactive power setting time has been reduced by 2 seconds compared to mode 1.
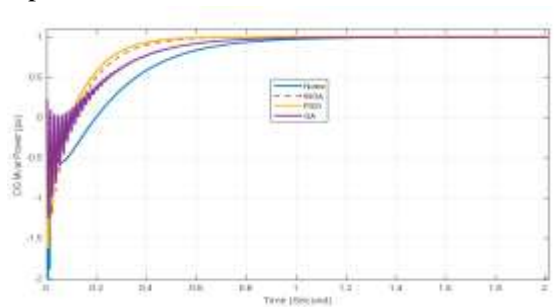

Fig 17: Generator`s reactive power with fixed wind speed in mode 2

7.3. Analysis of the Results of Simulation for Mode 3

The reference`s actual power of stator was extracted based on the wind's power-speed curve. The manufacturers of the variable-speed turbines/generators provide a power-speed curve for the turbine based on the aerodynamic properties of the blade and turbine, control considerations of the generator and wind speed changes, air density, and etc. They save the power-speed curve in a search table for controlling purposes. In order to extract the reference`s actual power, the generator speed was entered as an input into the search table. The search table output was the same as the stator or generator reference`s actual power. In the previous two modes,

it was assumed that the actual power control loop dynamic which was an electric dynamic, was fast enough, compared to the mechanical dynamics. In this case, for analysis and evaluation of the mechanical dynamics, the PI controller dynamic of the actual power could be ignored, and the measured actual power could be chosen as the reference value, and the integration error could be considered to be zero. However, in reality, due to the complexity of the behavior of the induction generator changes with the changes in wind speed, and the non-linear dynamic of induction flux, the effect of the controller dynamic cannot be ignored. The wind turbine control generally includes two main axes as the maximum absorbable mechanical power from the wind turbine and tracking the maximum power per different values of wind speed. The maximum absorbable mechanical power in each moment must be determined, and also, the turbine generator must be controlled in a way that in each moment, it can generate and track the mentioned maximum power. In this section, the optimization objective function included three components as a speed error, reactive power error, and active power error. The chart of the optimization convergence for the three intelligent search algorithms in 55 iterations out of 100 iterations was as below. In this regard, the minimum value of 2.62 was obtained in the 6th iteration for the gray wolf algorithm, the minimum value of 2.73 was obtained in the 6th iteration for the PSO algorithm, and the minimum value of 3.4 was obtained for the genetic algorithm. In fact, the genetic and PSO algorithms were trapped in the local minimum.
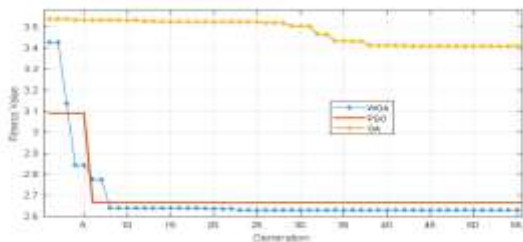

Fig 18: The three algorithms` convergence in mode 3

The step response to the generator speed with the optimum coefficients and the default algorithm coefficients was as below. In this regard, the gray wolf algorithm had a shorter setting time and it tended towards the nominal value after 18 seconds,

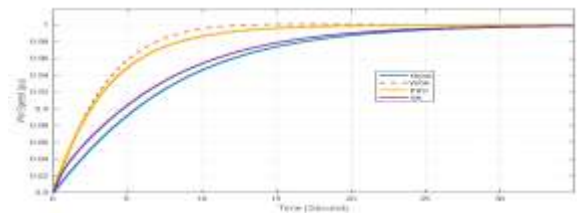while the genetic algorithm had a relatively slow setting time which was 41 seconds.

Fig 19: Generator`s speed with fixed wind speed in mode 3

The step response to the generated power was as below, which was similar to the previous section. The gray wolf algorithm had a shorter setting time and tended towards the per unit value in the fixed wind speed in the 22nd second. In this mode, also, the genetic algorithm setting time was longer than the PSO algorithm.
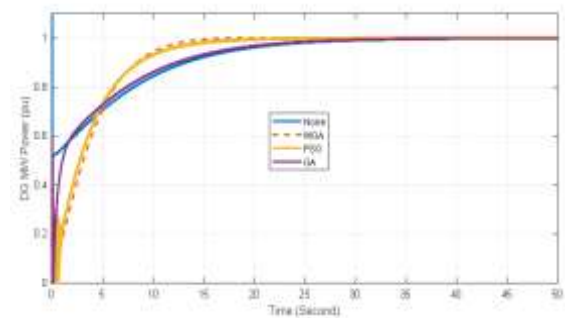

Fig 20: Active power with fixed wind speed in mode 3

The chart of step response to the reactive power generated with the optimum coefficients was as below. In this regard, the gray algorithm had a lower initial fluctuation compared to the other two algorithms, and the PSO algorithm had a higher overshoot and damping fluctuation than the other two algorithms.
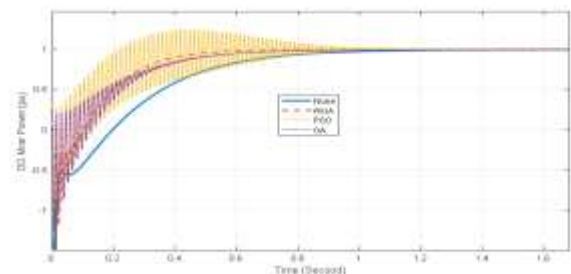

Fig 21: Reactive power with fixed wind speed in mode 3

7.4. Comparison of the Optimization Objective Functions in DFIG Power Control

The numeral results of the speed and power controllers coefficients for all three optimization models with the F1 to F3 objective functions have been provided in the below table. In this regard, in all three modes of optimization, the gray wolf algorithm error integral has been lower, and the speed controller coefficients in the F2 and F3 modes were almost the same.

Table 1
The control coefficients for the three modes

Case	Optimization Method	Speed Controller				Power Controller			
		P	I	P	I	P	I	P	I
Classic	-	0.015	0.294	0.010	0.441	0.872	3.229	0.888	3.801
F1	GWO	0.020	0.268	0.006	0.362	9.327	15.148	4.150	49.261
	PSO	0.008	0.262	0.005	0.362	0.608	96.174	0.444	94.834
	GA	0.436	0.439	0.034	0.368	8.896	49.136	13.270	32.826
F2	GWO	0.032	8.824	0.005	0.363	1.384	49.367	5.532	84.178
	PSO	0.029	8.824	0.006	0.366	26.004	47.810	2.731	114.018
	GA	0.375	7.413	0.041	0.433	2.258	35.031	6.662	15.176
F3	GWO	0.038	8.824	0.005	0.386	2.638	46.727	11.158	104.980
	PSO	0.456	8.824	0.006	0.386	18.367	61.698	9.851	25.270
	GA	0.787	8.805	0.082	0.584	21.031	89.983	20.251	77.783

7.5. The Effect of Wind Speed on Power Control with F3 Optimum Coefficients

In this section, the effects of random wind speed on the power controller performance with the F3 objective function optimum coefficients, were obtained according to (Yang et al. 2017). The results of the three optimization algorithms and default coefficients of controllers were compared. In the below chart, the speed error of the generator has been shown which, in spite of wind speed changes, has managed to control the nominal speed well, based on the reference power planned by the generator's power-speed curve. The controller setting time was shorter than the other methods using the gray wolf.
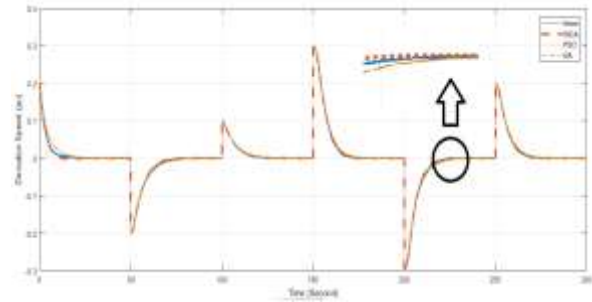

Fig 22: Speed deviation chart in mode 3 with the variable wind speed

The reactive power deviation chart was as below. The reactive power changes in the optimum mode had the lowest setting time with the gray wolf algorithm, which was indicative of the desirable performance of the controller with the wind speed changes.
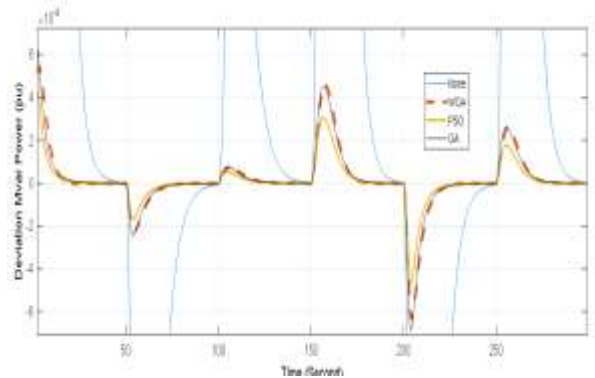

Fig 23: The reactive power deviation in mode 3 with variable wind speed

8. Conclusion

It is estimated that in the next 31 years, the global demand for energy would drastically increase, and the demand rate in 2131 would be much higher than the current demand. Today, the wind turbines are used for producing energy from the wind and converting it into electricity. based on the generators used in them, the wind turbines are divided into four classes, one of which has been considered in this study, which was the speed-variable pitch angle-variable turbine. In this type of turbines, the used generator is of doubly-fed induction type, which can actually control the generator speed. Numerous scientific efforts and research have been done by the researchers in order to maximize the power obtained from the wind. One of the widely used methods in the industrial systems controllers is the PID (Proportional Integral Derivative) method which is

known as a classic and widely used method. The practical use of it can be seen in a wind turbine. The wind turbine system, due to the non-linear behavior that shows, and existence of numerous external factors such as extra loads, wind speed fluctuations, etc. which may distort the system performance, would not respond equally to the linear controllers such as PID, and there is the possibility that after a while, the controlling coefficients must be set again, which is itself a problem. On the other hand, generally, there are several ideas to obtain the maximum power from wind energy, in most important of which, the wind turbine working area is divided into two sections as the area under the wind nominal speed and the area above wind nominal speed. And since the rotor speed is proportionate to the wind speed, and it is under its nominal value in the first zone, by setting the pitch angle as zero in this zone, the rotor speed was set proportionate to the wind speed, so that the edge speed would be fixed at 1.8. With this idea, the power also could have an optimum obtainable value under the nominal limit, at any wind speeds. In the second zone, in which the wind speed efficiency could reach the nominal value and exceeded it, the power has also reached its nominal limit. Moreover, with the increase in the wind speed, it was exceeded which has led to the damage to the electrical and even mechanical parts of the turbine. In order to obviate this problem, the status was changed in the second zone in a way that the generator speed was kept under its nominal value, and the pitch angle was controlled. Therefore, regarding this strategy, two controllers should be designed. One for the rotor speed and one for the pitch angle. On the other hand, since the DFIG could generate reactive power through the rotor to the stator for injecting to the grid, the reactive power consumed by the turbine can be also controlled. In the first zone, the rotor speed controller set the rotor speed to maximize the obtainable wind energy, while the pitch angle was kept zero. In order to do so, through the use of q component of the rotor which finally depended on its voltage, the controlling order was sent to the wind turbine system to adapt the rotor speed. In fact, firstly the rotor reference speed was calculated based

on the wind speed and knowing that the L value should be maintained at 1.8, and then, through the calculation of the existing error, the rotor speed controlling order was issued to the electrical system by the l_{qr} current. The reactive power in the DFIG could be controlled. This control was applied based on the direct component of the rotor current. Here, it was assumed that the optimum reactive power was about one-fourth of per unit. In the current study, the speed and reactive power controller coefficients in the tracking mode of maximum power were optimized by gray wolf optimizer algorithm and the results were compared with two different algorithms from the literature(GA and PSO), and the results of the effects of each algorithm on the generator response were revealed. Also, the importance of reactive power control and the speed in the optimization function was emphasized. The simulation results revealed the efficiency and advantages of the suggested control approach.

Consideration of various scenarios of noise and fault effects on the controller performance is suggested for further research on the subject.

References

[1] Padhy S., Panda S., "Application of a simplified Grey Wolf optimization technique for adaptive fuzzy PID controller design for frequency regulation of a distributed power generation system. Protection and Control of Modern Power Systems"; 2021, 6(2).

[2] Alhato M. M., Bouallègue S., Rezk H., "Modeling and Performance Improvement of Direct Power Control of Doubly-Fed Induction Generator Based Wind Turbine through Second-Order Sliding Mode Control Approach", Mathematics; 2020, 8.

[3] Soued S., Ramadan H. S., Becherif M., "Dynamic Behavior analysis for Optimally Tuned On-Grid DFIG Systems", Energy Procedia; 2019, 162. 339-348.

[4] Pradhan R., Majhi S. K., Pradhan J. K., Pati B. B, "Antlion optimizer tuned PID controller based on Bode ideal transfer function for automobile cruise control system", Journal of Industrial Information Integration; 2018, Eng J. 21 (5). 347-361.

[5] Rajesh K.S., Dash S.S., Rajagopal R., Sridhar R., "A review on control of ac microgrid", Renewable and Sustainable Energy Reviews; 2017, 71. 814-819.

[6] Liu W.Y., "A review on wind turbine noise mechanism and de-noising techniques", Renewable Energy; 2017,108. 311-320.

[7] Kahla S., Soufi Y., Sedraoui M., Bechouat M., "Maximum Power Point Tracking of Wind Energy Conversion System Using Multi-objective Grey Wolf Optimization of Fuzzy-Sliding Mode Controller", INTERNATIONAL JOURNAL of RENEWABLE ENERGY RESEARCH; 2017, 7(2).

[8] Yang B., Zhang X., Yu T., Shu H., Fang Z., "Grouped grey wolf optimizer for maximum power point tracking of doubly-fed induction generator based wind turbine", Energy Conversion and Management; 2017, 133. 427-443.

[9] He W, Ge S.S., "Vibration control of a nonuniform wind turbine tower via disturbance observer", IEEE/ASME Trans Mechatron; 2015, 20. 237–44.

[10] Osman A. A., El-Wakeel A. S., Kamel A., Seoudy H. M., "Optimal Tuning of PI Controllers for Doubly-Fed Induction Generator-Based Wind Energy Conversion System using Grey Wolf Optimizer", Journal of Engineering Research and Applications; 2015, 5(11). 81-87.

[11] Bekakra Y., Attous D. B., "Optimal tuning of PI controller using PSO optimization for indirect power control for DFIG based wind turbine with MPPT", International Journal of Systems Assurance Engineering and Management; 2013, 5(3). 219–229.

[12] Kristalny M., Madjidian D., Knudsen T, On using wind speed preview to; 2013, 21. 1191–8.

[13] Nam Y., Kien P.T., La Y., "Alleviating the tower mechanical load of multi-mw wind turbines with LQR control", Journal of Power Electronics; 2013, 13. 1024–31.

[14] Hwas A., Katebi R., "Wind turbine control using PI pitch angle controller", IFAC Conference on Advances in PID Control Brescia (Italy); 2012.

[15] Vieira J. P. A., Nunes M. V. A., Bezerra U. H., "Using genetic algorithm to obtain optimal controllers for the DFIG converters to enhance power system operational security", IREP Symposium Bulk Power System Dynamics and Control - VIII (IREP). Rio de Janeiro, Brazil; 2010, 1-9.

[16] Pao L.Y., Johson K.E. (2009). A tutorial on the dynamics and control of wind turbines and wind farms. In: American Control Conference. 2076–89.

[17] Zhao W., Stol K.A., "Individual blade pitch for active yaw control of a horizontal axis wind turbine", Proceedings of 45th AIAA Aerospace Sciences Meeting and Exhibit; 2007.

[18] Hau E. (2005) Wind turbines: fundamentals, technologies, application, economics. Springer.

[19] Johnson K.E., Pao L.Y., Balas M.J., Fingersh L.J., "Control of variable-speed wind turbine: Standard and adaptive technniques for maximizing energy capture", IEEE Control Syst Mag; 2005, 70–81.

[20] Battista D.H., Mantz R.J., Christiansen C.F., "Dynamical sliding mode power control of wind driven induction generators", IEEE Trans Energy Convers; 2000, 15. 451–7.